X-Ray Determination of Phonon Dispersion in Vanadium†

R. COLELLA AND B. W. BATTERMAN
Department of Materials Science and Engineering, Cornell University, Ithaca, New York 14850
(Received 22 September 1969)

Phonon frequencies along principal symmetry directions were measured in vanadium by means of thermal diffuse scattering of x rays. A polishing and annealing procedure was adopted which eliminated extra scattering associated with impurities. The dispersion curves have initial slopes in agreement with the measured elastic constants. We found no evidence of any irregularity at low frequencies in any of the dispersion curves and in the calculated frequency spectrum. A low-frequency peak in the frequency spectrum has been reported in two inelastic neutron-scattering experiments and was attributed to a Kohn effect. A Born–von Kármán model with seven-neighbor forces gave an adequate fit to the dispersion curves within experimental uncertainty. The derived interatomic force constants are not consistent with an axially symmetric model. The calculated frequency spectrum is in generally good agreement with the inelastic neutron determinations, but indicates the presence of more detailed structure. The high-energy tail observed in many experiments is not confirmed, nor does the $g(\nu)/\nu^2$ curve exhibit any hump in the low-frequency region.

I. INTRODUCTION

A STRONG interest has developed in the past few years in lattice dynamics of bcc transition metals. For elements of group V, the dispersion curves of niobium and tantalum have been determined by inelastic neutron-scattering experiments performed, respectively, by Nakagawa and Woods[1] and by Woods,[2] and it was found by these authors that a relatively large number of neighbors was needed to fit the dispersion curves to a Born–von Kármán model (eight for niobium and seven for tantalum). The phonon-dispersion relations of vanadium cannot be determined by conventional neutron-diffraction techniques, because its cross section for neutron scattering is almost totally incoherent. On the other hand, this unusual feature allows a rather direct measurement of the phonon frequency spectrum from inelastic neutron scattering.[3,4]

Vanadium, like niobium, has elastic constants such that the slope at the origin of the (001) L (longitudinal) mode is almost twice that of the (001) T (transverse) mode. Since the two curves, by symmetry, must coincide at the zone boundary, this would require the existence of long-range interactions which could only be determined by a direct measurement of the phonon-dispersion curves.

Several features of the experimentally determined neutron spectra are puzzling. Peretti *et al.*[5] give theoretical arguments for the possible existence of low-energy peaks in the frequency spectrum associated with the Kohn effect. This would be important if strong electron-phonon coupling played a significant role in vanadium's vibrational properties. A low-energy peak has been observed in two experimental determinations of the frequency spectrum at $\nu = 2\times10^{12}$ sec^{-1}.[4,6]

Although several of the experimental frequency spectra (via neutron scattering)[3,4] agree in general features with one another, detailed portions of the curves are in poor agreement. Some results show a high-energy tail which is difficult to explain theoretically. There is some feeling that this may be associated with impurities, or possibly multiphonon scattering.

One approach to resolving some of these ambiguities is to obtain a direct measurement of the individual phonon-dispersion curves which may be more sensitive to the above effects and from these determine an independent frequency spectrum. At present, the only means to do this is via the thermal diffuse scattering (TDS) of x rays. Preliminary measurements along the symmetry axes have been reported by Kashyap and Batterman[7] and by Pons-Corbeau and Jouffroy.[8]

In this work, the TDS of x rays was measured along the principal symmetry directions of the reciprocal lattice in single-crystal vanadium. The frequencies corresponding to a phonon wave vector are obtained from the absolute intensity of the thermal scattering at the appropriate scattering vector.

II. EXPERIMENTAL

Cu $K\alpha$ radiation from the point source of an x-ray tube was monochromatized by a doubly bent symmetric LiF crystal.[9] Typical working conditions were 35 kV, 15 mA. The monochromator had the Warren focusing, i.e., at the sample in the plane of incidence (horizontal) and focusing in the vertical plane at the counter. The

† Work supported by the U. S. Atomic Energy Commission.
[1] Y. Nakagawa and A. D. B. Woods, Phys. Rev. Letters **11**, 271 (1963).
[2] A. D. B. Woods, Phys. Rev. **136**, A781 (1964).
[3] G. Dolling and A. D. B. Woods, in *Thermal Neutron Scattering*, edited by P. A. Egelstaff (Academic, New York, 1965), p. 210.
[4] D. J. Page, Proc. Phys. Soc. (London) **91**, 76 (1967).
[5] J. Peretti, I. Pelah, and W. Kley, Phys. Letters **3**, 105 (1962).
[6] I. Pelah, R. Haas, W. Kley, K. H. Krebs, J. Peretti, and R. Rubin, in *Inelastic Scattering of Neutrons in Solids and Liquids*, (International Atomic Energy Agency, Vienna, 1963), Vol. II, p. 155.
[7] B. M. S. Kashyap and B. W. Batterman, Bull. Am. Phys. Soc. **12**, 282 (1967).
[8] J. Pons-Corbeau and J. Jouffroy, Bull. Soc. Fran. Mineral. Crist. **90**, 498 (1967).
[9] B. E. Warren, *X-Ray Diffraction* (Addision-Wesley, New York, 1969). See Chap. XI, for a general description of the principles involved in this experiment.

volume element (i.e., illuminated volume) in the region of reciprocal space investigated had linear dimensions of the order of one-tenth of the width of the Brillouin zone.

To eliminate air scattering, the specimen was kept in a chamber with Mylar windows filled with helium gas. In addition, lead baffles were mounted inside and outside the chamber to eliminate spurious scattering. This chamber was mounted on an Eulerian cradle which provided tilting movements needed for the measurement of the transverse modes. The incident and diffracted rays always made the same angle with the specimen surface so that no angularly dependent absorption correction was necessary. A correction was introduced to allow for different absorption in the Mylar windows at different tilting angles.

A proportional counter SPG-6 (General Electric) operated at 1870 V was used in this experiment, followed by a charge-sensitive preamplifier and a single-channel analyzer. The strong $K\alpha$ fluorescence from vanadium ($\lambda = 2.50$ Å) could be reduced to a negligible level by means of four aluminum filters 0.001 in. thick at the counter and by a careful adjustment of the first level of the single-channel analyzer. The adequacy of the four filters to eliminate the vanadium fluorescence was checked by ascertaining that a fifth foil reduced the weak TDS by an amount corresponding to that of pure Cu $K\alpha$ radiation. The upper level of the single-channel analyzer was adjusted to get rid of $\frac{1}{2}\lambda$ contributions. However, at the zone boundaries this short-wavelength contribution was sometimes so strong that electronic discrimination was inadequate. Figure 1 shows the pulse spectrum obtained by means of a multichannel analyzer at the zone boundary point (1.5, 1.5, 0) in reciprocal space corresponding to $\frac{1}{2}\lambda$ diffracting from the (330) reflection of vanadium. In the vicinity of the zone boundary, a Ni-Co balanced filter was used for certain dispersion curves to eliminate this $\frac{1}{2}\lambda$ contribution. In some cases, redundant measurements were made with the balanced filter far from the zone boundary, to check the reproducibility of previous measurements taken without the filters. The incident beam was monitored by measuring scattering from an amorphous material (polystyrene). These measurements were then put on an absolute basis by comparison with the integrated intensity from a powder standard of aluminum.

The powder specimen was prepared in the same manner as that used by Batterman, Chipman, and DeMarco[10] for the measurement of the atomic scattering factor of aluminum. Two diffraction lines (111)

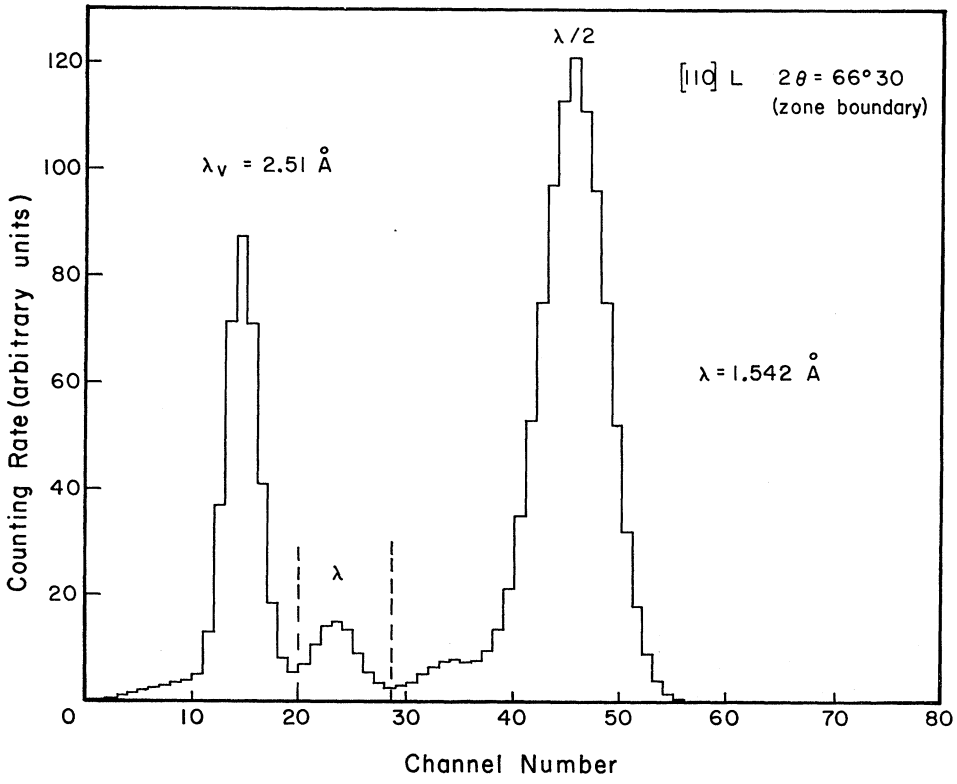

FIG. 1. Pulse-height spectrum from the proportional counter used in this experiment, at the point (1.5, 1.5, 0) in reciprocal space. The three peaks correspond (from right to left) to: $\frac{1}{2}\lambda$(Cu $K\alpha$), λ(Cu $K\alpha$), λ(V $K\alpha$) (fluorescence). The vertical dotted bars around the λ peak indicate the position of the window of the single-channel analyzer.

[10] B. W. Batterman, D. R. Chipman, and J. J. DeMarco, Phys. Rev. 122, 68 (1961).

and (200) were considered for the measurement of the incident beam, and an average value was adopted in the computations of the absolute TDS intensities. The values of the atomic scattering factors for aluminum were those measured by Batterman, Chipman, and DeMarco.[10] The anomalous dispersion corrections were taken from Cromer.[11] The TDS correction was evaluated using Chipman and Paskin's formula,[12] and it was found negligible for both lines.

It has been pointed out[13] that a LiF monochromator cannot usually be considered a mosaic crystal. The polarization of the monochromatized beam cannot therefore be calculated as for a mosaic crystal. This polarization, in our case, was evaluated by measuring the anomalous transmission of the monochromator beam through a single crystal of silicon in such a way that each polarization could be measured separately. A ratio for these two components of 0.629 was obtained, which is intermediate between the values for a perfect and a mosaic crystal (0.707 and 0.499, respectively). A total of three single crystals of high purity were used.[14] The surfaces used for the x-ray diffraction experiments were parallel to the (100), (110), and (111) lattice planes, respectively. A preliminary series of measurements gave dispersion curves which were not in agreement with the sound velocities for small q values. It was subsequently shown that this effect was due to hydrogen as an impurity.[15]

A polishing and annealing procedure was then suggested by Westlake[16] in order to eliminate hydrogen. Annealing at 800°C in vacuum (10^{-6} Torr) was believed to remove any hydrogen impurity, as suggested by resistometric measurements,[17] and in fact the (100) and (110) dispersion curves (longitudinal and transverse modes) exhibited the expected slopes at the origin.

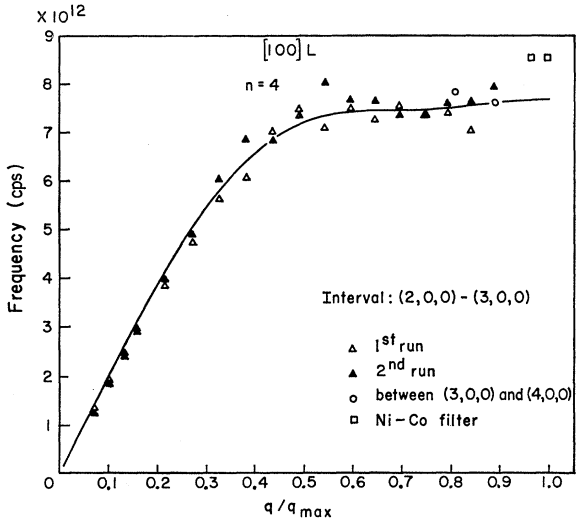

FIG. 2. Frequency versus q/q_{max} for the (100) L mode.

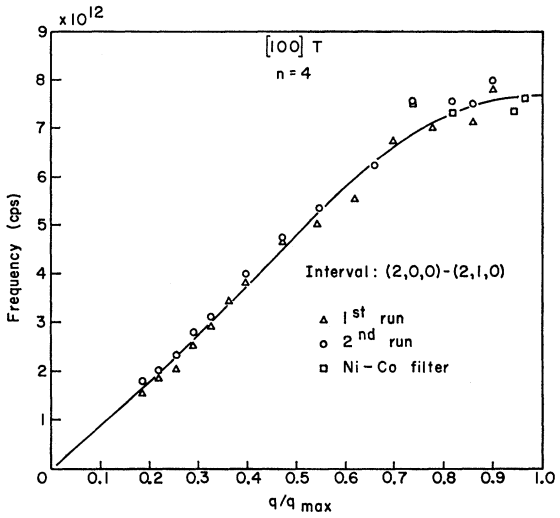

FIG. 3. Frequency versus q/q_{max} for the (100) T mode.

A strong extra scattering was detected, however, at $2\theta = 65°$ along the (111) L mode. This effect was noticed in three different samples, with different orientations. Two had the (111) planes parallel to the surface, while the third was cut parallel to (110). This extra intensity was rather diffuse, although the half-width of the peak on a θ–2θ scan was about 3°. It could not be identified with any vanadium-hydride reflections, which seems to rule out the role of hydrogen in this process. In all crystals, this effect was eliminated by etching the surface by means of a mixture (80:20) of HF and HNO_3 followed by rinsing with methyl alcohol. It was verified experimentally that the (100) and (110) dispersion curves were not detectably affected by this treatment.

The experimental dispersion curves are shown in Figs. 2–8. Because of the structure of the incident beam, the determination of the zero position of the counter was rather imprecise. Therefore, the correction to the abscissa was evaluated empirically by forcing the extrapolated dispersion curve for $q=0$ to go through the origin. The smooth curves are the result of a least-square fitting, based on a Born–von Kármán model up to seven neighbors. At the origin, they are forced to have the slope given by the sound velocity for the branch considered as measured by Alers[17] and Bolef.[18] The (100) crystal was used for the (100) L, (100) T, and (110) T_2 modes. For (110) T_1 and (110) T_2, the polarization is parallel to the ⟨110⟩ and ⟨100⟩, directions, respectively. The (110) crystal was used for the (110) L, (110) T_1, and (111) T modes as well as for the (111) L mode by tilting the crystal 35.3° so that the (111) direction coincided

[11] D. T. Cromer, Acta Cryst. **18**, 17 (1965).
[12] D. R. Chipman and A. Paskin, J. Appl. Phys. **30**, 1998 (1959).
[13] D. G. Westlake, Phil. Mag. **16**, 905 (1967).
[14] We are indebted to Dr. E. Greiner of the Bell Telephone Laboratories, Murray Hill, N. J., for kindly supplying the crystals.
[15] L. D. Jennings, Acta Cryst. **A24**, 472 (1968).
[16] D. G. Westlake (private communication).
[17] G. A. Alers, Phys. Rev. **119**, 1532 (1960).
[18] D. I. Bolef, J. Appl. Phys. **32**, 100 (1961).

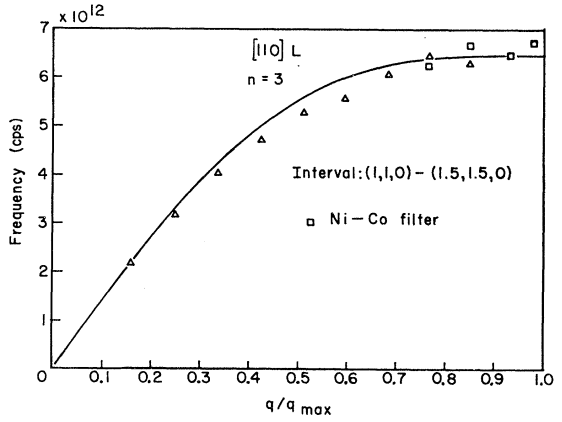

FIG. 4. Frequency versus $q/q_{\max}$ for the (110) L mode.

with the diffraction vector. In addition, the (111) L mode was measured on a crystal whose face is parallel to (111). The measurements on the (100) crystal were repeated on a freshly polished surface, as a check of reproducibility. The two sets are labelled as first and second run on Figs. 2, 3, and 6. Some points near the zone boundaries refer to measurements taken with the balanced Ni-Co filter, as indicated on the figures. As a further check on reproducibility for the (100) L mode, the intensity was also measured at two points between (3,0,0) and (4,0,0) and the corresponding frequencies have been plotted on the equivalent positions in the (2,0,0)–(3,0,0) region (Fig. 2). The ranges of the regions measured are shown in the figures.

III. TREATMENT OF EXPERIMENTAL DATA

The measured intensity is made up of different contributions which have to be evaluated separately. Electronic and cosmic background was measured daily, with the x-ray beam off, and was a rather constant 3 to 4 counts/min. This amounted to about 5% of the average intensity away from the Bragg nodes. The incoherent contribution (Compton scattering) was evaluated from the cross sections calculated by Freeman,[19] by interpolating between Ca and Fe. A proof of the reliability of such an interpolation can be obtained as follows[20]: If the same procedure is applied between Ca^+ and Fe^+, the value of V^+ which results from this interpolation is within 1% to the actual value V^+ calculated by Freeman. The fraction of the incoherent intensity is of the order of 50% of the measured intensities. The two-phonon TDS is evaluated in the Appendix, following a procedure suggested by Walker,[21] assuming that all the elastic waves are either longitudinal or transverse, and follow a simple dispersion law with different sound velocities for the longitudinal and the transverse modes. Details, and a table generally applicable for future calculations are given in the Appendix. TDS of order higher than 2 has been neglected. The fraction of second-order TDS is of the order of 5–10% of the total. The first-order TDS in electron units per atom from a single Bravais lattice is related to the frequency of the phonons by the well-known formula

$$I(\mathbf{S}/\lambda)=f^2e^{-2M}\frac{|\mathbf{S}/\lambda|^2}{m}\sum_j\langle E_{gj}\rangle\frac{\cos^2(\mathbf{S},\mathbf{e}_{gj})}{\nu_{gj}^2}, \quad (1)$$

where $\mathbf{S}/\lambda$ is the diffraction vector, f is the atomic scattering factor, M is the Debye-Waller factor, m is the mass of the vanadium atom, $\langle E_{gj}\rangle$ is the average energy of an harmonic oscillator associated with the phonon with wave vector g of the jth branch, and $\mathbf{e}_{gj}$ and ν_{gj} are, respectively, the direction of polarization and the frequency of the same phonon.

The atomic scattering factor and the real part of the anomalous dispersion correction are taken from Cromer and Waber[22] and Cromer,[11] respectively. The imaginary part of the dispersion correction has been calculated from the experimental value of the linear absorption coefficient for Cu $K\alpha$ radiation, given by Cooper.[23] The Debye-Waller factor has been calculated by using a Debye temperature of 325°K, which was obtained from the experimental frequency spectrum determined by Page.[4] This value is different from that calculated from our dispersion curves (374°K), but the over-all effect on the absolute frequency values is within the experimental error. Only phonons propagating along principal crystallographic directions ⟨100⟩, ⟨110⟩, and ⟨111⟩ have been taken into consideration. These phonons can be either longitudinal or transverse. The intensity at points in reciprocal space which lie on a radial line through the origin and a reciprocal-lattice point depends only on the longitudinal modes [$(\mathbf{S},\mathbf{e}_g)=90°$ for the two transverse modes] so that the summation in (1) contains only one term. In this way the longitudinal frequencies are ob-

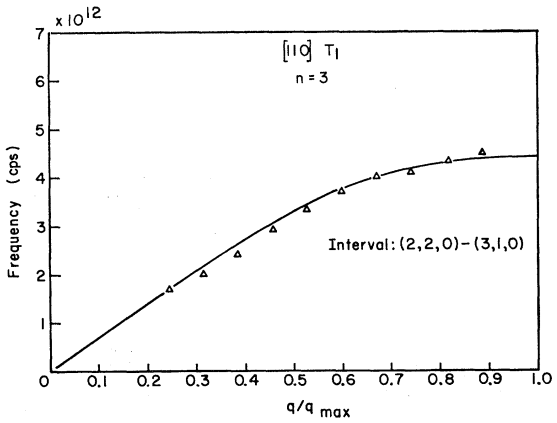

FIG. 5. Frequency versus $q/q_{\max}$ for the (110) T_1 mode (polarized parallel to a $(1\bar{1}0)$ direction.

[19] A. J. Freeman, Acta Cryst. **15**, 682 (1962).
[20] J. Pons-Corbeau, Compt. Rend. **264**, 478B (1967).
[21] C. B. Walker, Phys. Rev. **103**, 547 (1956).
[22] D. T. Cromer and J. T. Waber, Acta Cryst. **18**, 104 (1965).
[23] M. J. Cooper, Acta Cryst. **18**, 813 (1965).

tained. When TDS is measured along directions perpendicular to the straight line along which the longitudinal modes were measured, the summation in (1) is made up of two terms, one containing the unknown transverse frequency, the other one corresponding to the previously determined longitudinal mode. The longitudinal ν-versus-q modes were least-squared fitted to the analytical expression (2) (see Sec. IV) and from these the smooth ν values were used in (1) for the determination of the transverse frequencies. In principle, when the transverse frequencies are to be measured, it is not necessary to pick modes for which the direction of phonon propagation is perpendicular to the direction along which the longitudinal modes were measured. It is, however, convenient to adopt this procedure because the longitudinal contribution, which is an additional term to be subtracted from the total intensity, is minimized. An attempt to measure the (111) T mode on a (111) crystal along the $[1\bar{1}1]$ direction was unsuccessful because the longitudinal contribution to be subtracted off was too large (in light of experimental uncertainty) to make the difference meaningful.

Thus, the experimentally determined *transverse* frequencies are not independent data, but depend on the measured longitudinal modes. The contribution from the latter is usually small and for the purposes of the analysis to be described later, the transverse frequencies will be considered as independent data.

IV. ANALYSIS OF DISPERSION CURVES

It is well known that within the framework of the Born–von Kármán model, the dispersion curves can be analytically represented by Foreman and Lomer[24]:

$$(\nu_j^{hkl})^2=\frac{1}{4\pi m}\sum_{1}^{N}{}_n\,\phi_{nj}^{hkl}\left(1-\cos\frac{n\pi q}{q_{\max}}\right), \qquad (2)$$

where ν_j^{hkl} is the frequency of phonons of the jth branch propagating along the (hkl) direction, m is the atomic mass, the ϕ_{nj}^{hkl} are the interplanar force constants, and N is determined by the number of neighbors to be taken into account.

The interplanar force constants are linear combinations of the interatomic force constants. For the bcc lattice, the coefficients of the linear combinations are given by Woods *et al.*[25] up to five neighbors. Table I shows the values for the sixth and seventh neighbors, the notation for the interatomic force constants being that used by Squires.[26] The least-squares analysis has been based on the use of the expression (2), combined with Table I so that the data are related directly to the interatomic force constants. All the experimental data are simultaneously taken into account in the least-squares fitting giving the most probable set of inter-

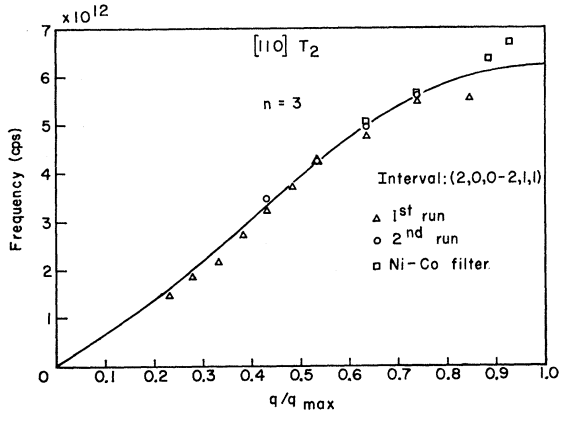

FIG. 6. Frequency versus $q/q_{\max}$ for the (110) T_2 mode (polarized parallel to a (001) direction.

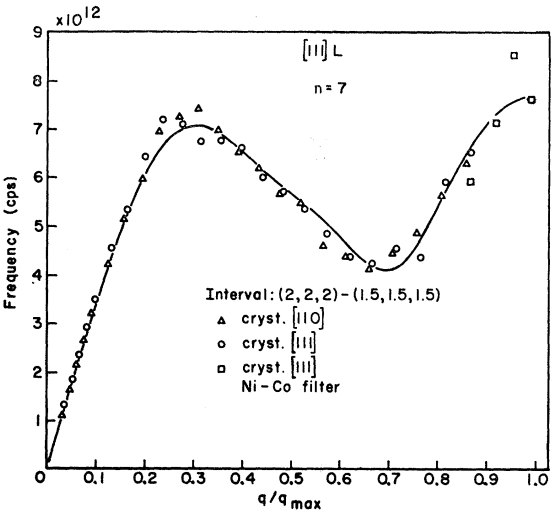

FIG. 7. Frequency versus $q/q_{\max}$ for the (111) L mode.

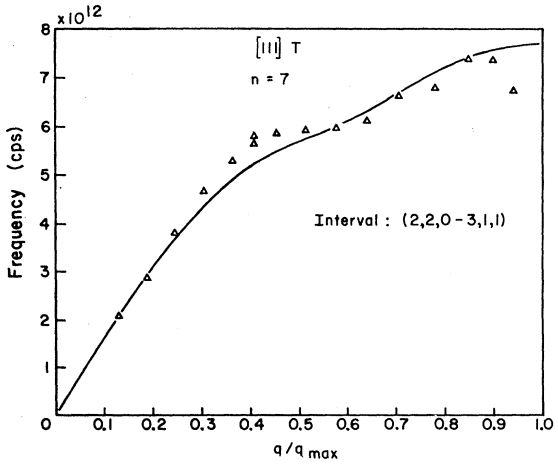

FIG. 8. Frequency versus $q/q_{\max}$ for the (111) T mode.

[24] A. J. E. Foreman and W. M. Lomer, Proc. Phys. Soc. (London) **B70**, 1143 (1957).

[25] A. D. B. Woods, B. N. Brockhouse, R. H. March, A. T. Stewart, and R. Bowers, Phys. Rev. **128**, 1112 (1962).

[26] G. L. Squires, Arkiv Fysik **25**, 21 (1963).

TABLE I. Linear combinations relating the interplanar force constants to the interatomic force constants (α,β) for the sixth and seventh neighbors in a bcc lattice. $\zeta_{\max}=q/q_{\max}$. n is the plane index.

Position of atom			$\frac{1}{2}a(4,0,0)$		$\frac{1}{2}a(3,3,1)$			
Branch	$\zeta_{\max}$	n	α_1^6 $\langle xx\rangle$	α_2^6 $\langle yy\rangle$	α_1^7 $\langle xx\rangle$	α_3^7 $\langle zz\rangle$	β_3^7 $\langle yz\rangle$	β_1^7 $\langle xy\rangle$
$[00\zeta]L$	1	1				8		
		3			16			
		4	2					
$[00\zeta]T$	1	1			8			
		3			8	8		
		4		2				
$[\zeta\zeta 0]L$	0.5	1			4	4	−8	
		2	2	2	4	4	8	
		3			4			4
$[\zeta\zeta 0]T_1$	0.5	1			4	4	8	
		2	2	2	4	4	−8	
		3			4			−4
$[\zeta\zeta 0]T_2$	0.5	1			8			
		2		4	8			
		3				4		
$[\zeta\zeta\zeta]L$	1	1			8	4		−8
		4	2	4				
		5			4	2	−8	4
		7			4	2	8	4
$[\zeta\zeta\zeta]T$	1	1			8	4		4
		4	2	4				
		5			4	2	4	−2
		7			4	2	−4	−2

atomic force constants. An imposed condition on the interatomic force constants is that they are consistent with long-wavelength elastic constants determined by Alers[17] and Bolef.[18] The results are given in Table II for seven neighbors. Suitable weights have been associated with the experimental points according to the statistical fluctuations of the counting rate and to the fraction of first-order TDS to the total intensity. The errors have been calculated assuming that there are no random errors in the $q/q_{\max}$ values and that the frequencies are determined to $\pm 5\%$. The solid curves in Figures 2–8 correspond to a fitting using up to seven-neighbor interatomic force constants. The n values indicated on each plot correspond to the number of planes necessary in the summation of Eq. (2) to include up to seven-neighbor interatomic force constants. For six and five neighbors the fitting becomes poorer, especially for the (111) modes.

The interatomic force constants have also been calculated in the case of seven neighbors in two steps, by a somewhat different procedure. First, the interplanar force constants in Eq. (2) were determined with the least-squares method on each individual dispersion curve as though they were all independent. Then a set of interatomic force constants was obtained from an overdetermined linear system of equations, by the least-squares method. In these least-squares analyses, the interplanar and the interatomic force constants were forced to be consistent with the elastic constants. The values obtained are also listed in Table II. It was found that the fitting was generally poorer in this case.

V. DISCUSSION

These interatomic force constants are far from satisfying the relationships required by an axially symmetric model,[27,28] which is an indication of a pronounced asphericity of the charge density, in agreement with the results of Weiss and DeMarco[29] on the $3d$ orbital population in vanadium. The frequency spectrum can be calculated from the interatomic force constants. A computer program developed by Raubenheimer and Gilat[30] and made available to us by Nicklow of ORNL, has been used for this purpose. The results are shown in Figs. 9 and 10 and are compared with the last (and probably the most accurate) experimental neutron determination by Page.[4] For Figs. 9 and 10, the interatomic force constants used are from the second and third columns, respectively, of Table II. Although in both cases there is fairly good agreement between the neutron- and x-ray-determined spectra, the agreement is certainly better in Fig. 10, where the interatomic force constants are those computed indirectly from the interplanar force constants. These, however, gave a poorer fit to the dispersion curves and therefore are believed to be less accurate. No explanation is available for such a discrepancy except that it may reflect the

TABLE II. Values of the interatomic force constants (dyn/cm) for a seven-neighbor model, obtained directly from the dispersion curves (left column), and via the interplanar force constants (right column).

Interatomic force constants	Direct fitting (dyn/cm)	Calculated from the interplanar force constants (dyn/cm)
$\alpha_1^1\langle xx\rangle$	10 872±380	10 534± 97
$\beta_3^1\langle xy\rangle$	7244±390	6305±141
$\alpha_1^2\langle xx\rangle$	6493±840	7129±257
$\alpha_2^2\langle yy\rangle$	−2148±530	−955±157
$\alpha_1^3\langle xx\rangle$	2994±280	2730± 79
$\alpha_3^3\langle zz\rangle$	−4686±420	−4494±128
$\beta_3^3\langle xy\rangle$	571±410	952±165
$\alpha_1^4\langle xx\rangle$	1435±360	1555± 90
$\alpha_2^4\langle yy\rangle$	286±230	420± 63
$\beta_1^4\langle yz\rangle$	−1151±240	−1527± 89
$\beta_3^4\langle xy\rangle$	1216±200	977± 51
$\alpha_1^5\langle xx\rangle$	9±210	−296± 62
$\beta_3^5\langle xy\rangle$	−123±350	263±100
$\alpha_1^6\langle xx\rangle$	−1389±610	−1343±136
$\alpha_2^6\langle yy\rangle$	341±310	660±110
$\alpha_1^7\langle xx\rangle$	−135±120	−94± 39
$\alpha_3^7\langle zz\rangle$	−360±160	−653± 62
$\beta_1^7\langle yz\rangle$	−431±170	−822± 49
$\beta_3^7\langle xy\rangle$	86±160	397± 52

[27] J. De Launay, in *Solid State Physics*, edited by F. Seitz and D. Turnbull (Academic, New York, 1956), Vol. 2, Sec. VII.
[28] G. W. Lehman, T. Wolfram, and R. E. DeWames, Phys. Rev. **128**, 1593 (1962).
[29] R. J. Weiss and J. J. DeMarco, Phys. Rev. **140**, A1223 (1965).
[30] L. J. Raubenheimer and G. Gilat, ORNL Report No. ORNL-TM-1425, 1966 (unpublished).

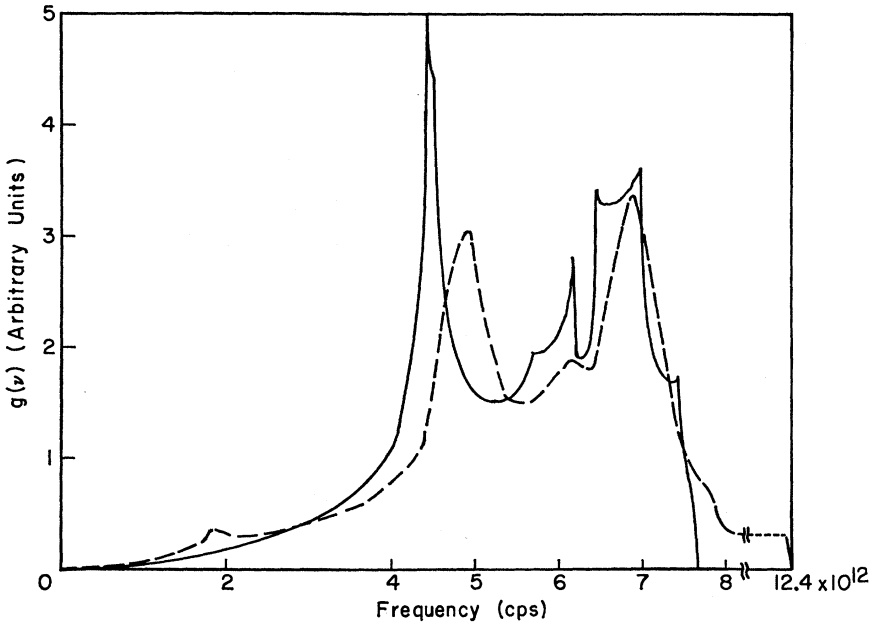

FIG. 9. Frequency spectrum of vanadium determined in this experiment from the interatomic force constants obtained from a least-squares fit to all the dispersion curves, i.e., those in Figs. 2–8. The dashed curve is Page's (Ref. 4) results from inelastic neutron scattering. Note the break in the abscissa for high frequencies.

experimental uncertainty in determining the dispersion curves.

The calculated spectrum does not show any evidence of a high-energy peak, as observed by Page[4] and other authors.[3] It is now believed that this high-energy tail might be due to improper correction for multiphonon processes.[31]

A low-energy peak has been observed in two previous neutron experiments[4,6] and attributed by Pelah *et al.* to a Kohn effect. The x-ray dispersion curves show no irregularities in the low-frequency region nor does the corresponding calculated frequency spectrum show any hump. The low-frequency region is experimentally the most accurate, since the thermal scattering is high here, and the extra contributions are a small fraction of the total measured intensity. It is concluded that if this low-energy peak is real, it must be associated with some unusual features of the surfaces of constant frequency far from the symmetry directions which have been investigated in this work.

The Debye temperatures Θ_M^{calc} (related to vibrational amplitude) calculated from the spectra in Figs. 9 and 10 are 367 and 374°K, respectively. These are in general agreement with the value $\Theta_M^{\text{expt}}=(366\pm25)$°K obtained by Brockhouse[32] from the temperature dependence (in the range 84–493°K) of the elastic incoherent neutron scattering from polycrystalline vanadium. The corresponding Θ_M's calculated from frequency spectra determined by inelastic neutron scattering are 323°K (calculated by Weiss and DeMarco[29] from Stewart and Brockhouse's[33] spectrum) and 325°K calculated from Page's[4] experimental results. Part of the difference between these and our results is probably associated with the low-frequency peak, in the case of Page's spectrum, which would tend to weight the lower frequencies more and this gives a lower Θ_M.

The specific-heat Debye temperature Θ_D^{calc} at 4.2°K calculated from our spectra in Figs. 9 and 10 is 383°K. This disagrees with the value $\Theta_D^{\text{expt}}=338$°K[34] obtained from the specific heat at 4.2°K.

Since the initial slope of our dispersion data agree well with elastic-constant measurements we would expect the corresponding Debye temperatures Θ_D^{calc} from our spectra to agree with Θ_E^{expt} determined by Alers[17] because in both cases these quantities are determined by the low-frequency modes. The values $\Theta_D^{\text{calc}}=383$°K from Figs. 9 and 10 and $\Theta_E^{\text{expt}}=388$°K from Alers bear this out. The agreement between these elastic-constant values and the discrepancy with the experimental specific-heat value of 338°K supports the hypothesis put forward by Alers[17] that "the low-temperature specific heat includes a contribution which varies as T^3 in addition to the lattice T^3 term." This additional T^3 term in the specific heat was hypothesized by Alers to explain the large discrepancy between $\Theta_E^{\text{expt}}=388$°K and $\Theta_D^{\text{expt}}=338$°K.[35]

VI. CONCLUSIONS

The dispersion curves of vanadium have been determined along symmetry directions through the mea-

[31] D. T. Keating (unpublished).
[32] B. N. Brockhouse, Can. J. Phys. **33**, 889 (1955).
[33] A. T. Stewart and B. N. Brockhouse, Rev. Mod. Phys. **30**, 236 (1958).
[34] W. S. Corak, B. B. Goodman, C. B. Satterthwaite, and A. Wexler, Phys. Rev. **102**, 656 (1956).
[35] This discrepancy has been attributed by J. A. Morrison and L. S. Salter [Phys. Letters **9**, 110 (1964)] to incorrect interpretation of specific-heat data.

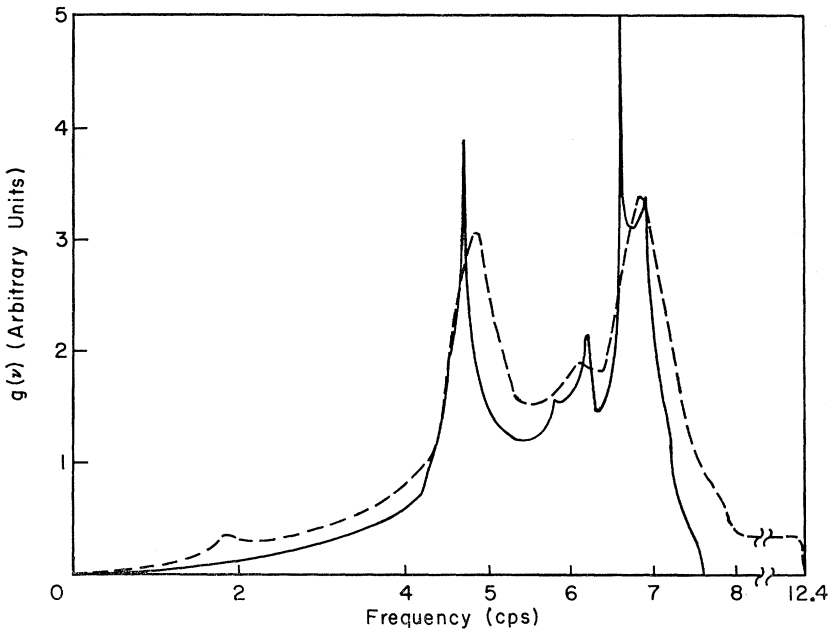

FIG. 10. Same as Fig. 9 but the interatomic force constants are derived from the interplanar force constants obtained from a least-squares fit to the individual dispersion curves.

surement of thermal diffuse scattering of x rays. These dispersion curves have slopes at the origin in agreement with the elastic constants determined by ultrasonic techniques. Within the experimental errors involved, the dispersion curves could be adequately fitted to a Born–von Kármán model with interactions extended out to seven neighbors. No irregularity was observed in the low-energy region of the dispersion curves which could be associated with the low-energy peak, in the frequency spectrum experimentally determined by Pelah *et al.*[6] and by Page[4] from inelastic neutron scattering. The interatomic force constants do not satisfy the relations required by an axially symmetric model, thus suggesting an appreciable asphericity of the electronic charge density, in agreement with the results obtained by x-ray diffraction.

The frequency spectrum calculated from the force constants is in generally good agreement with the inelastic neutron results. The present results seem to rule out the existence of a high-energy tail, observed by many authors,[3] and suggest that the low-energy peak observed in some of the experimental spectra, if it is not the result of spurious effects, must be associated with some unusual features of the surfaces of constant frequency off the symmetry axes in k space.

ACKNOWLEDGMENTS

We would like to express our appreciation to the U. S. Atomic Energy Commission for support of this project and also to the Advanced Research Projects Administration for the use of the central facilities of the Materials Science Center at Cornell University. The authors were aided considerably by consultations with Dr. C. B. Walker and Dr. D. T. Keating. We wish to thank Dr. R. Nicklow for use of his computer facilities to determine the frequency spectra from the measured force constants, and Dr. D. J. Page who kindly supplied the numerical values of his frequency spectrum.

APPENDIX: SECOND-ORDER THERMAL DIFFUSE SCATTERING

The intensity, in electron units, of thermal diffuse scattering due to two-phonon processes at the position $\mathbf{S}/\lambda$, is given by (see Ref. 9, Eq. 11.40):

$$I_2\left(\frac{\mathbf{S}}{\lambda}\right)=\frac{f^2e^{-2M}v_0}{2m^2}(KT)^2\left|\frac{\mathbf{S}}{\lambda}\right|^4\sum_{hkl}\int\sum_{jj'}\frac{\cos^2(\mathbf{S},\mathbf{e}_{gj})}{\nu_{gj}^2}\times\frac{\cos^2(\mathbf{S},\mathbf{e}_{g'j'})}{\nu_{g'j'}^2}dV \quad \text{(A1)}$$

(see Sec. III for explanation of symbols), where the summation over hkl is to be extended over all the contributing lattice nodes and v_0 is the volume per atom.

It has been assumed that the temperature is high enough so that the average energy associated with each wave is KT. For each node considered in the reciprocal lattice, Eq. (A1) has to be integrated over the overlapping volume of two spheres, of radius $g_{\max}$, one centered at the node hkl and the other at the tip of the $\mathbf{S}/\lambda$ vector (see Fig. 11).

In addition to the usual assumptions concerning the shape of the first Brillouin zone, crystal isotropy, and polarization of the normal modes,[9] we shall adopt two different sound velocities,[21] V_L for longitudinal and V_T

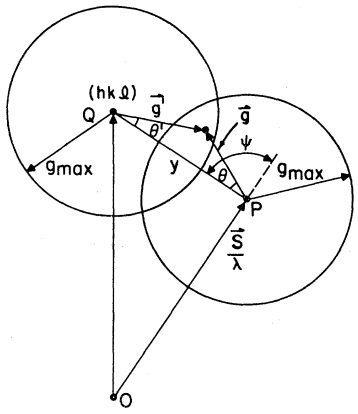

FIG. 11. Geometry of the calculation of the second-order diffuse scattering. The contribution from a lattice node Q is to be evaluated at the position P. The plane $(\mathbf{g},\mathbf{g}')$ does not, in general, coincide with the plane of the figure. Its azimuth with respect to the plane of the figure is called ϕ in the text.

for transverse phonons. These values have been averaged over the principal symmetry directions. Moreover, a simple dispersion law has been introduced[21] of the form $\nu = V(2g_{\max}/\pi)\sin(\pi g/2g_{\max})$, where ν is the frequency and V is either V_L or V_T.

It can be shown that the integral in Eq. (A1) can be decomposed into three terms:

$$L_1 = \frac{2K}{V_L{}^4}\int G(x)\frac{\cos^2\alpha\cos^2\beta}{z^2}d\cos\theta\, d\phi\, dx,$$

$$L_2 = \frac{2K}{V_L{}^2V_T{}^2}\int G(x)\frac{\cos^2\alpha\sin^2\beta+\cos^2\beta\sin^2\alpha}{z^2}d\cos\theta\, d\phi\, dx,$$

$$L_3 = \frac{2K}{V_T{}^4}\int G(x)\frac{\sin^2\alpha\sin^2\beta}{z^2}d\cos\theta\, d\phi\, dx,$$

where $K=\pi^4/16g_{\max}$, $x=g/g_{\max}$, $G(x)=x^2/[\sin^2(\frac{1}{2}\pi x)]$, $g=|\mathbf{g}|$, α and β the angles between $\mathbf{S}/\lambda$ and $\mathbf{g}$ and $\mathbf{S}/\lambda$ and $\mathbf{g}'$, respectively. θ and θ' are the angles between $\mathbf{QP}$ and $\mathbf{g}$ and $\mathbf{QP}$ and $\mathbf{g}'$, respectively. ϕ is the azimuth of the $(\mathbf{g},\ \mathbf{g}')$ plane; $Z=\sin[\frac{1}{2}\pi(x^2+\gamma^2-2x\gamma\cos\theta)^{1/2}]$, $y=|\mathbf{QP}|$, and $\gamma=g/g_{\max}$. If α and β are expressed in terms of θ,θ',ϕ, and ψ, and the integrations with respect to ϕ are carried out (over 2π) it turns out that

$$\begin{aligned} L_1 &= (2K/V_L{}^4)F_4,\\ L_2 &= (2K/V_L{}^2V_T{}^2)(F_2+F_3-2F_4),\\ L_3 &= (2K/V_T{}^4)(F_1-F_2-F_3+F_4), \end{aligned} \tag{A2}$$

TABLE III. Numerical values of the five integrals [Eq. (A4)] involved in the calculation of the second-order thermal diffuse scattering.

γ	10^2V_0	10^2V_1	10^2V_2	10^2V_3	10^4V_4
0.1	423.6	124.7	291.5	104.2	−196.9
0.2	221.2	63.65	152.7	53.72	−80.84
0.3	152.0	42.66	106.4	36.41	27.72
0.4	116.3	31.94	83.16	27.52	127.0
0.5	94.03	25.44	68.98	22.04	215.3
0.6	78.21	21.11	59.08	18.31	290.3
0.7	65.87	18.01	51.26	15.57	349.5
0.8	55.23	15.64	44.23	13.43	389.0
0.9	44.80	13.67	36.72	11.64	403.0
0.97	36.19	12.35	29.83	10.45	390.6
1.03	17.50	9.679	14.25	8.261	243.5
1.1	14.67	8.524	11.87	7.215	218.0
1.2	11.12	6.952	8.948	5.827	174.7
1.3	8.048	5.438	6.491	4.541	127.4
1.4	5.465	4.001	4.484	3.371	82.00
1.5	3.516	2.768	2.968	2.379	47.30
1.6	2.125	1.781	1.853	1.569	24.32
1.7	1.149	1.016	1.036	0.9215	10.38
1.8	0.4992	0.4624	0.4661	0.4328	3.137
1.9	0.1239	0.1196	0.1198	0.1156	0.4028
2.0	0.0	0.0	0.0	0.0	0.0

where

$$\begin{aligned} &F_1 = 2\pi V_0,\quad F_2 = 2\pi\cos^2\psi V_1+\pi\sin^2\psi(V_0-V_1),\\ &F_3 = 2\pi\cos^2\psi V_2+\pi\sin^2\psi(V_0-V_2),\\ &F_4 = 2\pi\cos^4\psi V_3+\pi\sin^2\psi\cos^2\psi\\ &\qquad\times(V_2+V_1-2V_3-4V_4)\\ &\qquad+\tfrac{3}{4}\pi\sin^4\psi(V_0-V_1-V_2+V_3), \end{aligned} \tag{A3}$$

and

$$\begin{aligned} V_0 &= \int G(x)\frac{dt\,dx}{z^2},\qquad V_1 = \int G(x)\frac{t^2dt\,dx}{z^2},\\ V_2 &= \int G(x)\frac{t'^2dt\,dx}{z^2},\qquad V_3 = \int G(x)\frac{t^2t'^2dt\,dx}{z^2},\\ V_4 &= \int G(x)\frac{tt'(1-t^2)^{1/2}(1-t'^2)^{1/2}}{z^2}dt\,dx, \end{aligned} \tag{A4}$$

$$t=\cos\theta,\quad t'=\cos\theta' = \frac{y-x\cos\theta}{(x^2+\gamma^2-2x\gamma\cos\theta)^{1/2}}.$$

The five integrals V_0, V_1, V_2, V_3, and V_4 have been evaluated numerically for a number of values of the parameter $\gamma=y/g_{\max}$ between 0 and 2 (see Table III) in one of the two halves of the common region of the two spherical Brillouin zones centered on Q and P, such that $|\mathbf{g}|\leq|\mathbf{g}'|$. For each contributing node $Q(hkl)$, the angle ψ and the parameter $\gamma=y/g_{\max}$ are determined, and the second-order TDS can be easily calculated from (A2), (A3), and from Table III. Table III can be used for any crystal with one atom per cell, to which the approximations involved can be applied.